A&A 453, 517–524 (2006)
DOI: 10.1051/0004-6361:20054697

Astronomy & Astrophysics

VLT/NACO near-infrared imaging and spectroscopy of N159A in the LMC HII complex N159⋆,⋆⋆

G. Testor[1], J. L. Lemaire[2,3], D. Field[4], and S. Diana[2,3]

[1] LUTH, UMR 8102 du CNRS, Observatoire de Paris, 92195 Meudon, France
e-mail: gerard.testor@obspm.fr
[2] LERMA, UMR 8112 du CNRS, Observatoire de Paris, 92195 Meudon, France
[3] Université de Cergy-Pontoise, 95031 Cergy Cedex, France
e-mail: jean-louis.lemaire@obspm.fr
[4] Department of Physics and Astronomy, Århus University, 8000 Århus C, Denmark
e-mail: dfield@phys.au.dk

Received 16 December 2005 / Accepted 9 March 2006

ABSTRACT

We present near-infrared imaging and spectrocopic observations of the HII region N159A (∼10 pc) in the giant star-forming region N159 (50 pc) in the LMC. N159A was observed in the J and Ks bands at high spatial resolution ∼0.2″ using the ESO Very Large Telescope UT4 (VLT), equipped with the NAOS adaptative optics system. Our data reveal the morphology of this region in unprecedented detail. The protostar P2, one of the first YSOs of Class I identified in the LMC is now resolved in two YSO candidates. The ultracompact HII region LI-LMC 1501W is found to be a tight cluster embedded in a compact HII region ionised by a late O source. A new multiple system composed of a tight star cluster and an YSO candidate, all embedded in a compact nebular region (0.4 pc) is also detected at the north-east edge of N159A. The stellar population of the whole N159A region appears composed of two main stellar populations, one with an age ≤3 Myr and the other one with a large range of age (300 Myr–10 Gyr). Using spectroscopy, one of the two exciting O stars in the HII region N159A is classified O5-O6.

Key words. galaxies: Magellanic Clouds – ISM: individual objects: N159A – stars: formation – stars: pre-main sequence – HII regions

1. Introduction

The Large Magellanic Cloud (LMC) is rich in HII regions and young OB associations. Because of its known and relatively small distance (50 kpc) (Storm et al. 2004), its face-on position relatively free from foreground extinction, it is well suited to the study of both individual stars and very compact objects as well as global structures. It is an ideal laboratory in which to study the formation and evolution of massive stars in a low metallicity environment.

Understanding the characteristics of massive stars and their interaction with their environment is a key problem in astrophysics. Such interactions are represented particularly by massive young stellar objects (MYSOs), ultracompact (UC) and compact (C) HII regions. The UCHII regions represent the earliest phase in which a new-born massive star can be detected by its ionising radiation. UCHII regions might evolve further into compact and classical HII regions (Wilcots 1994a). An area rich in young objects is found in the LMC in the 30 Doradus region. Southwards from this region, at a distance of ∼600 pc there is a chain of Henize (1956) giant HII regions namely N158, N160, N159 extending from the north to the south. It is believed that the star formation process started in 30 Doradus, and N159 lies at the still quiescent part of the 30 Doradus complex (Israel et al. 1996).

N159 is associated with the most important concentration of molecular gas in the LMC (Jones et al. 1986; Brooks & Whiteoak 1997; Johansson et al. 1998) and the emission is composed of three distinct GMCs, known as N159E, N159W and N159S. Recent CO observations of these GMCs are described by Fukui (2005). In N159 the first extragalactic YSO labelled P1 was discovered by Gatley et al. (1981). The region also contains the first extragalactic type I OH maser (Caswell & Haynes 1981) and a H_2O maser (Scalise & Braz 1981). Using a 5″ spatial resolution a second YSO labelled P2 was discovered by Jones et al. (1986) in N159A.

A high resolution 5 GHz radio map of N159 (Hunt & Whiteoak 1994) shows continuum features numbered #1 to #5. They have also been imaged at 3 and 6 cm with ATCA by Indebetouw et al. (2004) who found a radio source superposing the feature #5 which is assumed to be ionised by an O7 star (Martin-Hernandez et al. 2005).

N159 has been recently observed using Spitzer IRAC bands (3.5, 4.5, 5.7 and 7.9 μm) by Jones et al. (2005) who classify the protostar P2 as a Class I YSO with an age of $\sim 10^5$ yr and a luminosity of $(3-5) \times 10^3\ L_\odot$. The authors find no evidence for a red supergiant population.

An optical nebular study of N159 was performed by Heydari & Testor (1982) who discovered the first compact HII region N159-5, later named HEB (High Excitation Blob), being ionised by young massive stars just leaving their parental molecular

⋆ Based on observations obtained at the European Southern Observatories, El Paranal, Chile.

⋆⋆ Table 3 is only available in electronic form at the CDS via anonymous ftp to cdsarc.u-strasbg.fr (130.79.128.5) or via http://cdsweb.u-strasbg.fr/cgi-bin/qcat?J/A+A/453/517

Table 1. Log of photometric VLT/NACO observations.

Id.	Filter	Expo. $t(s) \times n$	Mode	Date	Seeing ($''$)
N159A	Ks	20×9	S54	9/10/2004	0.6–0.9
	J	10×30	–	10/10/2004	–
	Ks	20×20	–	11/10/2004	–
	J	30×30	–	–	0.9–1.2
S9109	J	1×4	–	10/10/2004	0.6–0.9
	K	1×4	–	–	–

cloud. A detailed study of N159-5 and its environment is found in Meynadier et al. (2004).

The region of special interest here is the HII region N159A. This region located in N159W is also named NGC 2079. N159W is thought to be ionised by five O5V stars (Bollato et al. 2000). The centre of the nebula contains the source DD13 (Dufour & Duval 1975) which is likely to be the major ionising source, of type O3–O6 (Conti & Fitzpatrick 1991). From optical stellar photometry of the region, DD13 is in fact composed of two stars of spectral type O5–O6V and O7–O8V (Deharveng & Caplan 1991). Heydari-Malayeri & Testor (1982) and Deharveng & Caplan (1991) found a visual extinction for N159A in a range of 1–4.5 mag.

In N159A, Comeron & Claes (1998) found two UCHII candidates at 15 μm named LI-LMC 1501W and LI-LMC 1501E corresponding to the feature #5 (Hunt & Whiteoak 1994) and P2 (Jones et al. 1986) respectively. As no peak in radio (1.4 and 2.4 GHz) has been found, Jones et al. (2005) conclude that LI-LMC 1501E = P2 is not an UCHII region but a YSO that may produce ionising radiation, and that it is not an embedded O star.

LI-LMC 1501E and 1501W are associated with N159-Y2, a Herbig Ae/Be cluster (Nakajima 2005). The fact that N159-Y2 harbours embedded massive stars suggests ongoing star formation.

In this paper we present VLT images and spectroscopy of N159A through J and Ks filters using adaptive optics which provided high spatial resolution images. Section 2 describes the observations and data reduction and presents the $J-Ks$ photometry toward the N159A region. In Sect. 3 we examine the morphology of N159A and discuss its stellar population. A detailed description of the three young, reddened and compact multiple systems in N159A is given. The results are summarized in Sect. 4.

2. Observations and data reduction

NIR observations of N159A were obtained at the ESO VLT during October 2004. Images and spectra were obtained using NACO composed of the Nasmyth Adaptative Optics System (NAOS) and the High Resolution IR Camera and Spectrometer (CONICA). The detector was a 1026×1024 SBRC InSb Alladin 3 array. We used the camera mode S54 with a field of view $54'' \times 54''$ with a pixel size of $0.05273''$ corresponding to 0.0132 pc at the distance modulus of 18.5 for the LMC (Cole 1998). As reference source for wavefront sensing we used the bright star #205 of $V = 14.29$ mag (Deharveng & Caplan 1991) located at the center of N159A. The conditions were photometric and the seeing ranging from 0.65 to $1''$ in the visible. After subtraction of the average dark frame each image was divided by the normalized flat field image. The data were reduced with the ESO software packages MIDAS and ECLIPSE.

Table 2. Log of the VLT/NACO long-slit spectroscopic observations.

Id.	Date	Slit (mas)	Expo. $t(s) \times n$	Mode	$\lambda/\delta\lambda$	Seeing ($''$)
a	10/10/2004	172	100×10	S54-4-SHK	500	0.6-0.9
b	–	–	100×20	–	–	–

2.1. Imaging

Images were obtained through J and Ks filters (Table 1). The autoJitter mode was used: that is, at each exposure, the telescope moves according to a random pattern in a $6'' \times 6''$ box. The mean PSF measured on several stars in the J-band was $\sim 0.20''$ slightly increasing at the sides of the images following the decreasing Strehl ratio as the distance from the reference star from AO increases.

2.2. Spectroscopy

Spectroscopy was performed with the same camera in the mode S54-4-SHK (broad-band filter) giving a linear dispersion of 1.94 nm/pixel and a spatial scale of 54 mas/pixel. Two long slit spectra (Table 2) were taken, one (a) (PA = 49.°2) crossing N159A7 and #78 (Fig. 1) and the other (b) (PA = 303°) crossing N159A5 and N159A6. The slit width was 172 mas and the spectral resolution ~500. For each exposure the detector integration time (DIT) was 100 s. Five exposures were obtained for (a) and ten for (b). In order to remove telluric absorption features a star with a similar airmass was observed as the telluric standard. Spectroscopy was reduced with the MIDAS software package LONG.

2.3. Photometry

From the J and Ks images the instrumental magnitudes of the stars detected were computed using DAOPHOT/ALLSTAR (Stetson 1987) in a field of $48.''6 \times 48.''6$. The photometric calibration of our instrumental magnitudes was obtained using the standard star S9109 (Persson et al. 1998) as a reference star and the mean atmospheric extinction coefficients used at ESO. From the mean of the individual observations of S9109 we derived our correction constants with a standard deviation of ±0.03 mag. In Table 3 (electronic form) the astrometry and the $J - K$ photometry with photometric errors are given. The conversion of pixel coordinates to α and δ for J2000.0 was obtained using the star 205 (Deharveng et al. 1991) as reference. The relative position of our stars are accurate to around $0.1''$. Our photometry has detected 181 stars but we have taken into account only the sources having values both in J and K, which explains that some numbers are skipped over in Table 3. Figure 1 shows the stars identified by a number. Stars #76 and #78 correspond to a 2MASS point source of $4''$ spatial resolution (Table 4). This table lists the observed positions and spatial resolution published in the literature of the components of N159A studied below. The colour conversion was derived comparing the colour excess $(J-K)_{\rm NACO}$ of our brightest reddened sources N159A5, N159A7 and the blue O stars #76 and #78 integrated in a $4''$ aperture with the $(J - K)_{\rm 2MASS}$ of the same sources in 2MASS. We obtained the relation $(J-K)_{\rm 2MASS} = 1.02 \pm 0.03 (J-K)_{\rm NACO} + 0.03$. The integration of the bright stars #76 and #78 with faint stars in the same aperture gives $J = 13.45$ and $K = 13.02$ which is compared with

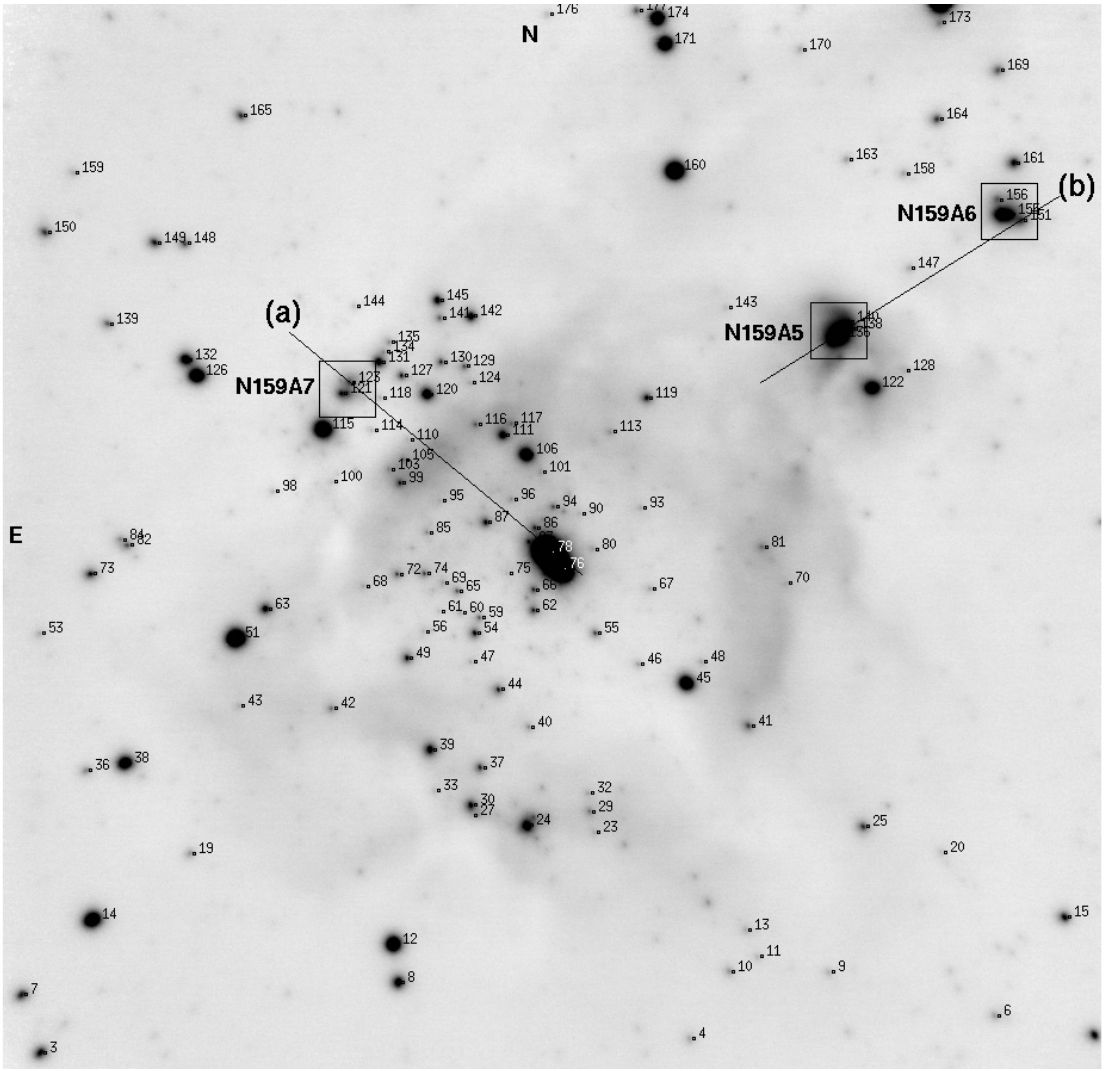

Fig. 1. Finding chart (*J* filter) for the stars detected in N159A. The numbers refer to Table 3. The areas containing the compact sources are outlined. The lines labelled **a)** and **b)** correspond to the two locations of the slit used in the spectroscopic mode. The central stars #76 and #78 correspond to DD13. The total field size corresponds to 48.6″ × 48.6″.

$J = 13.37$ and $K = 12.99$ in the 2MASS survey. The comparison shows a systematic magnitude offset of about +0.1 ± 0.02 for *J* and +0.03±0.05 for *K*s. However, it shows a strong dispersion in the range 0.05–1 mag for isolated fainter stars. This dispersion is not due to a lack of colour conversion but to the low spatial resolution of 2MASS (4″) that seems not well adapted for crowded fields such as N159A. Table 3 also contains, when available, the *BV* photometry obtained by Deharveng & Caplan (1992).

3. Results and discussion

3.1. Morphology of N159A

A composite *JK*s colour image of N159A clearly shows three well resolved compact and reddened sources as well as the two stars #76 and #78 forming DD13 (Fig. 2).

3.1.1. The compact sources

The first compact source N159A7 is in the direction of P2 (Jones et al. 1986), the second one N159A5 in the direction of Hunt & Whiteoak's (1994) object #5 (Table 4) and the third one N159A6, N-W of N159A is newly discovered. This latter presents no optical counterpart in Heydari & Testor (1982) but one IR point source numbered #59 in Jones et al. (1986). The three sources appear to be complex systems and their areas are

Table 4. Positions and spatial resolution of sources published in the literature associated with N159A.

Ident	α(2000)	δ(2000)	Spatial res. (″)
Source 59[jh]	5 39 36.61	−69 46 06.03	5
Feature 5[hw]	5 39 37.60	−69 46 11.50	8
B0540-6946(5)[i]	5 39 37.50	−69 46 10	1–2
LI-LMC 1501E[cc]	5 39 41.90	−69 46 16	3
LI-LMC 1501W[cc]	5 39 37.50	−69 46 14	3
Protostar P2[jw]	5 39 41.90	−69 46 11.12	2
2MASS source[c]	5 39 40.09	−69 46 19.6	4

[hw] Hunt & Whiteoak (1994), [cc] Comeron & Claes (1998), [c] Cutri et al. (2000), [i] Indebetouw et al. (2004), [jh] Jones et al. (1986), [jw] Jones et al. (2005).

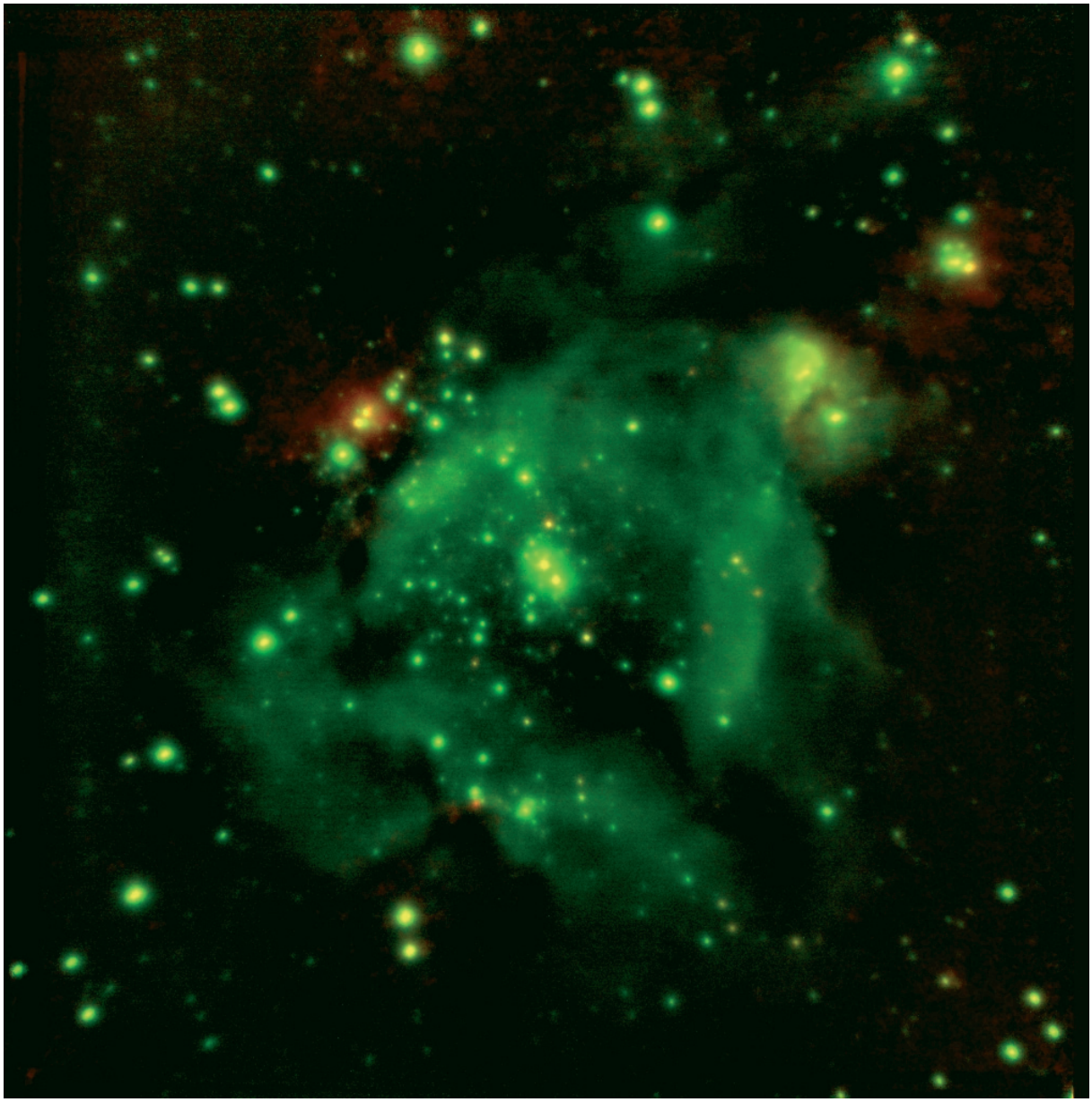

Fig. 2. *JK* colour composite image of LMC N159A (*K*s = red, *J* = green) showing the regions N159A7, N159A6 and N159A5 around DD13. North is up and east left. The field size is 54″ × 54″.

outlined in a box of 2.48″ × 2.48″ (Fig. 1). In this paper these regions containing the sources will be named from east to west N159A7, N159A5 and N159A6 (Fig. 1). The numbering is chosen in order to follow the labels of Hunt & Whiteoak (1994) features (#1–#5) (Fig. 3). The size of the box was chosen to be intermediate between the Spitzer IRAC spatial resolution ∼2″ (Surace et al. 2005) and the point spread function of ∼3″ at 15 μm (Comeron & Claes 1998).

3.1.2. Infrared colours

Figure 4 shows a $J - K$ versus K colour diagram. The reddening track for O stars is plotted assuming a total visual extinction, $A_V = 5.8E(J - K)$ (Tapia et al. 2003), $A_K = 0.112A_V$ (Rieke & Lebofsky 1985). It was derived using as reference the O star #76. This star has an intrinsic colour $(J-K)_0$ of ∼−0.16 from Lejeune & Shaerer (2001). Some of their isochrones with $Z = 0.008$ are overplotted. The diagram appears to reveal at least two stellar populations. This is obtained when the isochrones are shifted by reddening amounts of +0.41 and −0.25 mag along the colour and K magnitude axis. The first one is a young population of dwarf and giant OB stars which appears to be fitted with the 3 Myr isochrone. The second one is a clump of red giant stars around $K = 18$ and $J - K = 0.90$ in the K magnitude range of 16.8–19.2 mag expanding in the age range of 300–10 Gyr and corresponding to masses between ∼1 $M_\odot$ and 3 $M_\odot$. Most of the stars lying beyond the 10 Gyr isochrones and in the range of 3–300 Myr isochrones are likely to represent stars situated deeper in the molecular cloud. The stars located at the extreme right of the HR diagram, such as #151, #121 and #123, are the YSOs discussed below. Apart the YSO objects, the faint source #27 ($J = 20.02$) clearly seen on the composite image (Fig. 2) is the reddest ($J - K = 3.20$) and is probably a very young object. If we take into account the criterion $K \leq 13$ mag used in Nakajima et al. (2005) no supergiant population is found in our $J - K$ vs. K colour diagram.

Table 5. Selected compact multiple sources in N159A.

Ident	α(2000)	δ(2000)	J	$J-K$	Other source designations
N159A7					P2[jw], LI-LMC 1501E[cc]
121	5 39 41.96	−69 46 11.99	17.74	4.22	
121a[c]	5 39 41.92	−69 46 12.40	18.33		
123	5 39 41.90	−69 46 11.52	18.11	4.80	
123a[c]	5 39 41.97	−69 46 11.50	19.40		
N159A6					59[jh]
151	5 39 36.17	−69 46 4.35	17.91	3.44	
153	5 39 36.32	−69 46 4.27	16.91	0.99	
154[c]	5 39 36.21	−69 46 4.00	19.30	1.56	
155	5 39 36.28	−69 46 4.30	17.05	1.77	
156	5 39 36.34	−69 46 3.64	18.28	0.75	
157[c]	5 39 36.16	−69 46 3.99	19.10		
N159A5					#5[hw], LI-LMC 1501W[cc]
133	5 39 37.80	−69 46 9.90	17.86	1.99	
136	5 39 37.75	−69 46 9.70	17.04	1.73	
137	5 39 37.73	−69 46 9.41	17.50	1.38	
138	5 39 37.65	−69 46 9.40	18.56	2.01	
140	5 39 37.67	−69 46 9.05	18.50	1.90	
DD13[dd]					204, 205[dcl]
76	5 39 40.09	−69 46 19.76	14.68	0.21	
78	5 39 40.20	−69 46 18.99	13.93	0.45	

[c] Magnitudes derived by integration in a circular aperture.
[cc] Comeron & Claes (1998); [dd] Dufour & Duval (1975); [dcl] Deharveng et al. (1992); [hw] Hunt & Whiteoak (1994); [jh] Jones et al. (1986); [jw] Jones et al. (2005).

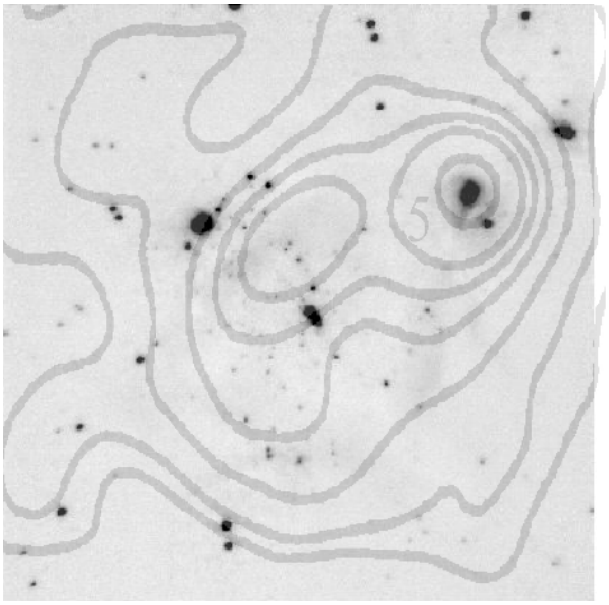

Fig. 3. Gray-scale image of N159A (K-band) overlaid with the 5 GHz radio contours from Hunt & Whiteoak (1994). Their feature #5 is indicated.

3.1.3. N159A5

N159A5, identified in Fig. 1, contains a tight cluster formed by the stars #133, #136 and #137 bordered by two fainter stars #138 and #140 to the N-W as shown in detail in Fig. 5. All the components are embedded in a nebulosity of diameter 1.9″ ∼ 0.50 pc. In Fig. 1 two northern and southern faint nebular extensions are seen, probably belonging to a larger structure in N159A. The J and K magnitudes corresponding to the different components are listed in Table 5. Star #136 coincides with star #230 of $V = 18.89$, $B-V = 0.46$ (Deharveng et al. 1992) and the radio source BO540-6946(5) (Indebetouw et al. 2004) (Table 4). The 5 GHz radio peak of the feature #5 (Hunt & Whiteoak 1994) west of P2 in Jones et al. (2005) is clearly associated with the Comeron & Claes (1998) source 1501W observed at 15 μm (Table 4). Therefore Jones et al. (2005) conclude that N159A5 is certainly a CHII region with one or more OB stars rather than a UCHII region (Comeron & Claes 1998). According to Martin-Hernandez et al.'s (2005) Fig. 4 based on the size of the nebula, N159A5 with a diameter of 0.50 pc might be classified at the frontier of CHII and HII regions (CHII/HII). N159A5 overlies a 6 cm radio peak (Indebetouw et al. 2004) as well as a 3.5 μm peak (Jones et al. 2005). A single 1D-spectrum (Fig.7) was extracted by summing a pixel range containing #133, #136 and the eastern edge of #137 along the 172 mas slit width **(b)**. The Br_γ and He I 2.058 μm intensity distribution along the slit is shown in Fig. 6. The spectrum (Fig. 7) shows a ratio HeI 2.112 μm/Br_γ of 0.021. According to Hanson et al. (2003) this ratio indicates that the CHII is ionised by a late O type source. This is in agreement with Martin-Hernandez et al. (2005) who found from the $N_{\rm Lyc}$ flux that the ionising source could be an O8V star. The HeII 2.185 μm absorption line is not detected. If we assume that N159A5 is mainly populated by OB stars, its extinction $A_{\rm V}$ is in a range of 8–12 mag (Fig. 4).

3.1.4. N159A6

In the frame shown in Fig. 5, N159A6 appears as a cluster of at least 6 stars embedded in a nebulosity of a total diameter of 1.8″ = 0.45 pc in the K-band. N159A6 contains two bright stars #153 $J = 16.91$ $J-K = 0.99$ and #155 $J = 17.09$, $J-K = 1.74$ separated only by 0.31″ and to its northern edge three faint stars #156, #154 and #157. On the western edge 0.7″ from #155 we find a very bright and red star #151 $J = 17.96$, $J-K = 3.41$. Table 5 lists the J and K magnitudes of the different components.

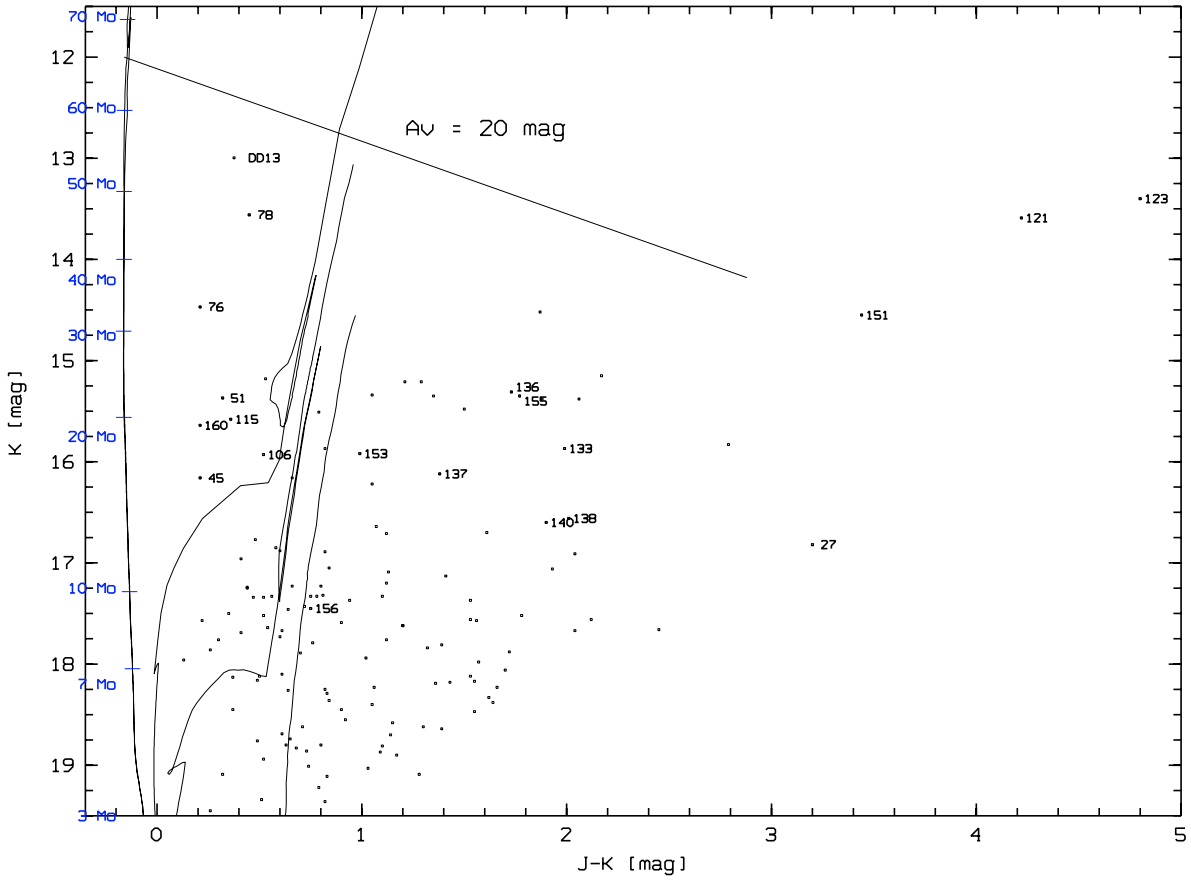

Fig. 4. *K* vs. $J-K$ colour magnitude diagram for the point sources detected in N159A. *From the left to the right* are overplotted the 3 Myr, 300 Myr, 1 Gyr and 10 Gyr isochrones (extinction-free). The reddening vector ($A_V \sim 20$ mag) is shown by a line. Some masses between 3 $M_\odot$ and 70 $M_\odot$ are marked with a tick on the 3 Myr isochrone. The 2MASS point source [5 39 40.09 −69 46 19.6] associated with DD13 (#76 + #78) is plotted (left on the upper HR diagram).

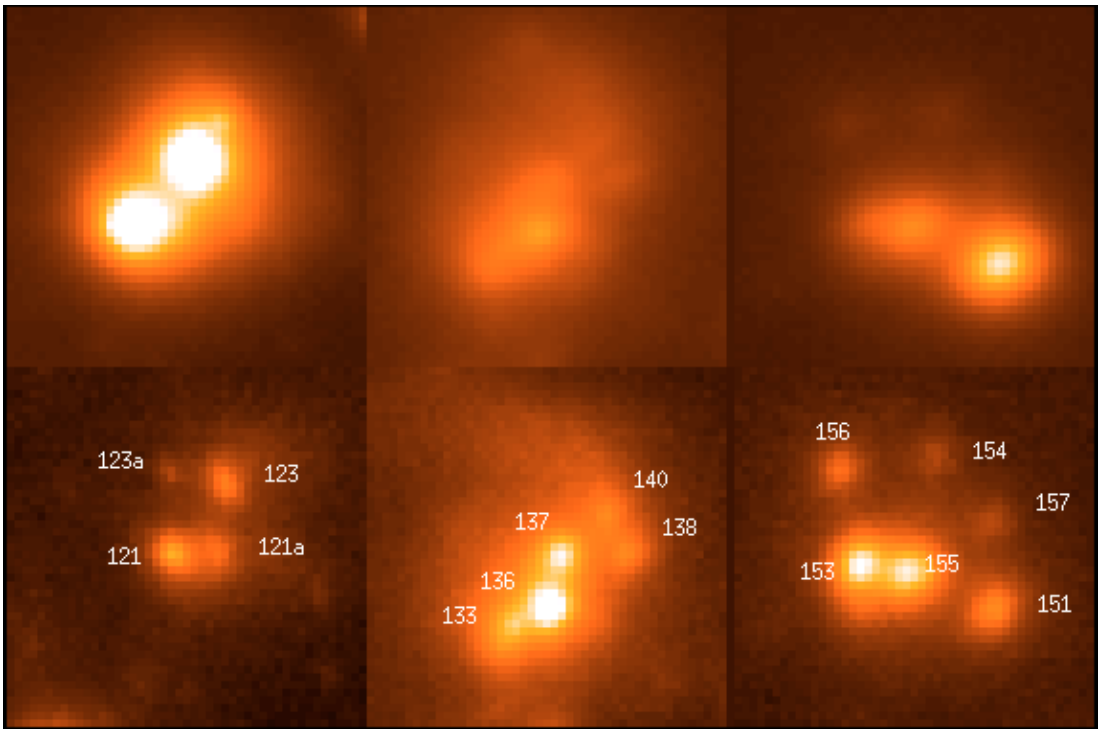

Fig. 5. Fields from east to west of N159A7, N159A5 and N159A6 in the band *J* (down) and *K*s (up). The intensity scale of the *K*s images is divided by a factor 12 compared to the *J* images in order to avoid saturation. The stars are labelled according to Table 5. Each field size is 2.″48 × 2.″48 (0.6 pc × 0.6 pc).

N159-A6 coincides in position with source No. 59 (Table 4) of $J = 15.27$ and $J - K = 2.09$ (Jones et al. 1986). It also corresponds to Deharveng et al.'s (1992) star #240 of $A_V = 2.3$ mag, which they assumed to be a very young object. In Jones et al. (2005) N159A6 overlies a peak at 3.5 μm of the Spitzer IRAC band 1 image of spatial resolution ∼2″. This peak covers all of the N159A6 region. According to Fig. 11 of Jones et al. (2005) with colours [5.7]–[7.9] μm = 1.80 and [3.5]–[4.5] μm = 0.55, this peak appears to be an HII region. Taking in the whole diameter (∼0.45 pc), the colour–colour diagram of Martin-Hernandez et al. (2005) shows that N159A6 is a CHII/HII region. At the location of N159A6 no peaks at 1.4 GHz, 2.4 GHz (Marx et al. 1997) or 5 GHz (Hunt & Whiteoak 1994) (Fig. 3) are found, while in Comeron & Claes (1998) a faint 15 μm emission is possibly detected. The absence of radio emission is compatible with the spectral energy distribution (SED) of the YSO P2 (Jones et al. 2005) and the star #151 could be a YSO that we label N159A6-151. The N159A6 region appears to be formed by an HII region containing five embedded stars ($1 < J - K < 1.8$) and the new YSO N159A6-151. The spectrum (b) crossing N159A6-151 (Fig. 7) shows the emission lines Brγ and H_2 2.121 μm. In this spectrum the He I 2.113 μm line is not detected. The Br_γ intensity distribution along the slit is shown in Fig. 6.

3.1.5. N159A7

N159A7 is composed of two stars, labelled #121 and #123, separated by 0.57″ in the J-band. Two faint features #121a and #123a are found, one to the west 0.26″ distant from #121 and the other to the east at 0.36″ from #123 (Fig. 5). All these components are embedded in a diffuse nebula of diameter 0.55 pc. In the K-band the stars #121 and #123 of about the same magnitude are very bright and highly reddened. Their FWHM corresponds to the point spread function determined with DAOPHOT, that is, ∼0.20″ or 0.05 pc. Table 5 gives the J and K magnitudes of the different components of N159A7. N159A7 lies north of the Deharveng & Caplan (1991) B1V star #217 ($V = 16.16$, $B - V = 0.04$) who suggested that #217, an Hα emission line star, is associated with P2 and could be a Herbig Ae/Be star. From our image it is clear that P2 is not associated with star #217, in agreement with Jones et al. (2005) who give a magnitude $J = 15.29$ and $J - K = 3.13$ for their unresolved source P2. In our K band the nebulosity of N159A7 reaches a total diameter of ∼1.6″ = 0.40 pc (Fig. 5) with a slight extension to the west. This nebulosity matches up with P2 and LI-LMC 1501E. Comeron & Claes (1998) classify P2 as a UCHII. This is in contradiction with Jones et al. (2005) who conclude that P2 is not an embedded O star but a Class I YSO. Our high resolution observations show that P2 is in fact formed by two stellar components, N159A7-121 and N159A-123, each of which could be a YSO candidate. In our spectrum (a), which crosses star #123 (Fig. 1), no He 2.113 μm line is detected (Fig. 7) signifying again that there is no O star (Hanson et al. 2002), in agreement with Jones et al. 2005. Our spectrum shows H_2 concentrated on star #123 with a faint extension towards #78 at a distance of 3″ and a very red continuum as seen in Rubio et al.'s (2005) spectrum of the unresolved P2. The Br_γ and He I 2.113 μm intensity distribution of N159A7-123 along the slit is shown in Fig. 6.

3.1.6. The central exciting stars

Stars #76 and #78 form the region DD13 (Fig. 1) and are reported in Conti et al. (1991) as responsible for the ionisation of the N159A nebula as a whole. This assumption seems strengthened by the location of the bright hot stars #51, #115 and #160 outside the nebula. DD13 is classified as an O3–O6 source in Conti et al. (1991). In Deharveng & Caplan (1991) stars #76 and #78 are classified as O7–O8 and O5–O6 respectively. A spectrum of star #78 (Fig. 7) shows the NIII 2.115 μm line. The presence of the HeII 2.185 μm absorption line is also detected as well as an emission feature of CIV at 2.083 μm. This star according to Bik et al. (2005) should be an early O star of type O5–O6, in agreement with Deharveng & Caplan (1991). For stars #76 and #78 ($J - K = 0.21$ and 0.45) we derive an A_V of 2.15 and 3.54 mag respectively higher than in Deharveng & Caplan (1991) who give 1.2 and 1.4.

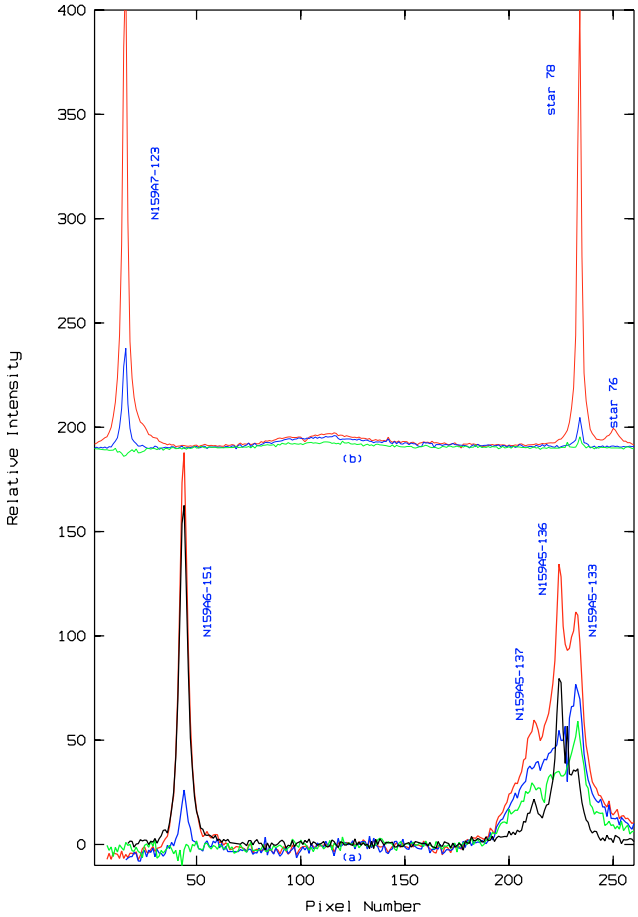

Fig. 6. *Upper frame*: intensity distribution along the slit **a)** of 13.7″ length crossing N159A7-123 and star #78. In red the Brγ line is plotted without subtraction of a nearby continuum while in blue the continuum is subtracted. The green line represents the intensity distribution of the He 2.058 μm line after continuum subtraction. Lower frame: intensity distribution along the slit **b)** of 13.7″ length crossing N159A5-133, 136, the edge of #137 and N159A6-151: Brγ line without nearby continuum subtraction (red line), with subtraction (blue line). The distribution of the nearby continuum is plotted (black line) as well as the He 2.058 μm line with continuum subtraction. The orientation of the slits **a)** and **b)** is shown in Fig. 1.

4. Conclusions

We present high-resolution (0.2″) JK VLT photometry of the N159A region with the detection of three deeply embedded multiple compact systems. These systems labelled N159A5,

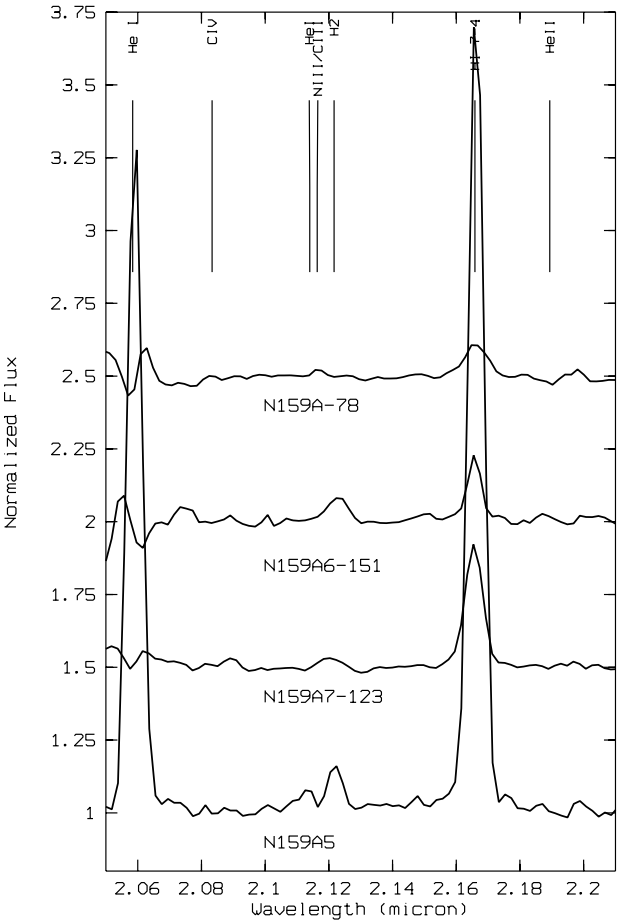

Fig. 7. *K*-band normalized spectra of the main central ionising source of N159A-78, N159A7-151 and N159A6-123 at top. Each 1D spectrum is extracted from **a)** or **b)** by summing a pixel range along the slit corresponding to 0.2″, 0.4″ and 0.5″ respectively. The bottom normalized spectrum N159A5 corresponds to a pixel range in **b)** of 2″ allowing to integrate N159A5-133, N159A5-136 and N159A5-137. The spectra are plotted in the range 2.05–2.21 μm.

N159A6 and N159A7 are analysed using imaging and spectroscopy. The results can be summarized as follows:

In N159A we have detected 133 stars in both the J and K bands. The colour–magnitude diagram may be interpreted to show a young population with an age ≤3 Myr and an older population with a large age range of 300 Myr to 10 Gyr. The diagram also shows very red objects ($2.40 < J - K \leq 4.80$), among them the three YSOs (N159A7-121, N159A7-123 and N159A6-151). No supergiant stars are found in N159A.

N159A5 (0.5 pc) is classified as a CHII/HII region containing a cluster of at least five stars. Spectroscopy shows that the main ionising source in N159A5 is a late O star.

N159A6, a new detection, is formed by two objects contained within a diameter of 0.5 pc. The first object is also a CHII/HII region containing about five stars. The second object, located to the south-east at the edge of the HII region, is a stellar object with a strong colour excess of $J - K = 3.4$. We classify this as a YSO.

N159A7 corresponding to P2, previously classified as YSO I, is in fact composed of two main bright, reddened stellar components #121 ($J - K = 4.19$) and #123 ($J - K = 4.77$), both of which we also classify as YSOs.

The very red object #27 ($J = 20.02$, $J-K = 3.2$) found south of N159A is most probably a further very young object.

From spectroscopy, #78 one of the two central O stars responsible for the ionisation of N159A, is classified as type O5–O6.

Our detection of unsuspected multiple compact young systems embedded in diffuse nebular regions clearly supports the idea that N159A represents an earlier stage of evolution than other regions in 30 Dor. However, higher spatial resolution at 0.08″–0.012″, possible with the S13 or S27 cameras, is still required to improve our knowledge of these multiple systems in one of the most interesting star-forming region in the LMC.

Acknowledgements. We thank the anonymous referee for his careful reading of the manuscript and comments to improve the paper.

References

Bollato, A., Jakson, J., Israel, F., Zhang, X., & Kim, S. 2000, ApJ, 545, 234
Bik, A., Kaper, L., Hanson, M. M., & Smits, M. 2005, A&A, 440, 121
Brooks, K., & Whiteoak, J. 1997, MNRAS, 291, 395
Caswell, J. L., & Haynes, R. F. 1981, MNRAS, 194, 33
Cole, A. A. 1998, ApJ, 500, L137
Conti, P., & Fitzpatrick, E. 1991, ApJ, 373, 100
Comeron, F., & Claes, P. 1998, A&A, 335, L13
Cutri 2003 University of Massachusetts and Infrared Processing and Analysis Center (IPAC) California institute of technology
Deharveng, L., & Caplan, J. 1991, A&A, 259, 480
Deharveng, L., Caplan, J., & Lombard, J. 1992, A&AS, 94, 359
Dufour, R. J., & Duval, J. E. 1975, PASP, 87, 769
Gatley, I., Becklin, E. E., Hyland, A. R., & Jones, T. 1981, MNRAS, 197, 17
Fukui, Y. 2005, IAU Symp., 227, 328
Hanson, M., Luhman, K., & Rieke 2002, ApJS, 138, 35
Henize, K. G. 1956, ApJS, 2, 315
Heydari-Malayeri, M., & Testor, G. 1982, A&A, 111, L11
Hunt, M., & Whiteoak, J. B., 1994, PASAu, 11, 68
Indebetouw, R., Johnson, K., & Conti, P. 2004, AJ, 128, 2206
Israel, F. P., Maloney, P. R., Geis, N., et al. 1996, ApJ, 465, 738
Johansson, L., Greve, A., Booth, R., et al. 1998, A&A, 331, 857
Jones, T. J., Hyland, A. R., Straw, S., et al. 1986, MNRAS, 219, 603
Jones, T., Woodward, M., Boyer, M., Gehrz, R., & Polomski, E. 2005, ApJ, 620, 731
Lejeune, T., & Shaerer, D. 2001, A&A, 366, 538
Martin-Hernandez, Vermej, R., & van der Hulst, J. M. 2005, A&A, 433, 205
Marx, M., Dickey, J. M., & Mebold, U. 1997, A&A, 126, 325
Meynadier, F., Heydari-Malayeri, M., Deharveng, L., et al. 2004, A&A, 422, 119
Nakajima, Y., Kato., D., Nagata., T., et al. 2005, AJ, 129, 776
Persson, S., Murphy, D., Krzeminski, W., Roth, M., & Rieke, M. 1998, AJ, 116, 2475
Rieke, G., & Lebofsky, M. 1985, ApJ, 288, 618
Rubio, M., & Barba, R. 2005, IAU 227 Symp. (poster)
Scalise, E., & Braz, M. A. 1981, Nature, 290, 36
Stetson, P. B. 1987, PASP, 99, 191
Storm, J., Carney, B. W., Gieren, W. P., et al. 2004, A&A, 415, 531
Surace, J.A,. Wang, Z., Willner, S., et al. 2005 Spitzer News Views of the Universe, ASP Conf. Ser.
Tapia, M., Persi, P., Roth, M., et al. 2003, MNRAS, 339, 44
Wilcots, E. M. 1994a, AJ, 107, 1338